THE JOURNAL OF BIOLOGICAL CHEMISTRY VOL. 281, NO. 16, pp. 11074–11081, April 21, 2006

Real-time Enzyme Dynamics Illustrated with Fluorescence Spectroscopy of *p*-Hydroxybenzoate Hydroxylase*

Received for publication, January 20, 2006 Published, JBC Papers in Press, February 21, 2006, DOI 10.1074/jbc.M600609200

Adrie H. Westphal[‡§], Andrey Matorin[‡], Mark A. Hink[‡§], Jan Willem Borst[‡§], Willem J. H. van Berkel[‡], and Antonie J. W. G. Visser[‡§¶1]

From the [‡]Laboratory of Biochemistry, Wageningen University, Dreijenlaan 3, 6703 HA Wageningen, the [§]MicroSpectroscopy Centre, P. O. Box 8128, 6700 ET Wageningen, and the [¶]Department of Structural Biology, Faculty of Earth and Life Sciences, Vrije Universiteit Amsterdam, De Boelelaan 1085, 1081 HV Amsterdam, The Netherlands

We have used the flavoenzyme *p*-hydroxybenzoate hydroxylase (PHBH) to illustrate that a strongly fluorescent donor label can communicate with the flavin via single-pair Förster resonance energy transfer (spFRET). The accessible Cys-116 of PHBH was labeled with two different fluorescent maleimides with full preservation of enzymatic activity. One of these labels shows overlap between its fluorescence spectrum and the absorption spectrum of the FAD prosthetic group in the oxidized state, while the other fluorescent probe does not have this spectral overlap. The spectral overlap strongly diminished when the flavin becomes reduced during catalysis. The donor fluorescence properties can then be used as a sensitive antenna for the flavin redox state. Time-resolved fluorescence experiments on ensembles of labeled PHBH molecules were carried out in the absence and presence of enzymatic turnover. Distinct changes in fluorescence decays of spFRET-active PHBH can be observed when the enzyme is performing catalysis using both substrates *p*-hydroxybenzoate and NADPH. Single-molecule fluorescence correlation spectroscopy on spFRET-active PHBH showed the presence of a relaxation process (relaxation time of 23 μs) that is related to catalysis. In addition, in both labeled PHBH preparations the number of enzyme molecules reversibly increased during enzymatic turnover indicating that the dimer-monomer equilibrium is affected.

Single-molecule fluorescence spectroscopy applied to proteins or nucleic acids have allowed direct observations of molecular properties, individual reaction steps, or intermediates that are otherwise hidden in conventional, ensemble experiments (1–5). These techniques have been developed for freely diffusing molecules as well as for surface-bound systems. A powerful approach is single-pair fluorescence resonance energy transfer (spFRET),[2] in which the resonance energy transfer efficiency from the donor to the acceptor of a doubly labeled system is used to distinguish subpopulations with different transfer efficiencies caused by different relative distances and orientations of donor and acceptor molecules arising from conformational changes (see for example Refs. 1, 2, and 6–8). Single-molecule fluorescence detection techniques have resulted in measurements of single enzyme turnovers of, among others, nuclease (9), horseradish peroxidase (10), ribozyme (11), exonuclease (12), and F_0F_1-ATP synthase (13, 14).

A spectacular breakthrough in single-molecule fluorescence detection of flavoenzymes was reported for cholesterol oxidase, in which single enzymatic turnovers were observed in real-time by monitoring the redox state via FAD (flavin) fluorescence (3, 4). The cholesterol oxidase was confined in an agarose gel preventing the enzyme diffusing away, but allowing free exchange of much smaller sized substrates and products. The flavin cofactor of cholesterol oxidase is nonfluorescent in the reduced state and slightly fluorescent in the oxidized state. Therefore, the successive "on-times" and "off-times" reflect the redox cycle and enzymatic turnover of the enzyme. Statistical analysis of multiple single-molecule trajectories revealed a detailed picture of reaction rate fluctuations and memory effects related to previous turnovers.

Despite the impressive results on cholesterol oxidase and more recently dihydroorotate dehydrogenase (15), flavoenzymes in general are not the easiest systems for single-molecule fluorescence studies. The flavin molecule bound in flavoenzymes has unfavorable photophysical properties: an intrinsic high triplet yield and in most cases low molecular brightness due to severe quenching of fluorescence (16–18). Another approach to overcome these limitations is to use a second, strongly fluorescent donor label that can communicate with the flavin via spFRET. Due to changes in the overlap of spectral cross-sections of flavin and donor label the donor fluorescence can be used as a sensitive antenna for the redox state and enzymatic activity of the flavoenzyme. The label can be designed in such a way that spFRET to the flavin will only affect the donor fluorescence when the flavin is in the oxidized state, whereas in the reduced state there is much less spectral overlap. Single-molecule fluorescence detection can thus provide insight in the conformational dynamics of single flavoenzymes in relation to catalysis.

We illustrate this approach using the dimeric flavoprotein *p*-hydroxybenzoate hydroxylase (PHBH, EC 1.14.13.2), a prototype for enzymes involved in the monooxygenation of an aromatic substrate (19). PHBH catalysis involves two half-reactions (Fig. 1) that occur in different active sites of the monomer. In the first half of the catalytic cycle, the FAD cofactor is reduced by NADPH in response to *p*-hydroxybenzoate binding and $NADP^+$ is released. In the second part of the reaction cycle, the reduced form of the enzyme-substrate complex reacts with oxygen to form a labile flavin (C4a)-hydroperoxide species, which attacks the substrate aromatic ring. During PHBH catalysis, the isoalloxazine ring of the FAD moves *in* and *out* of the hydroxylation pocket (20, 21). In the oxidized state, the flavin swings *out* for the reaction with NADPH (22–24). Upon reduction, the flavin moves to the *in* position, which is required for the oxygen reactions (25, 26). This *closed* conformation protects the flavin (C4a)-hydroperoxide from solvent and allows efficient substrate hydroxylation. Some PHBH mutants have been shown to stabilize an *open* conformation with solvent access to the active site (24, 26). This conformation of the enzyme is unreactive with

* This work was supported by a VLAG postdoctoral fellowship (to A. M.). The costs of publication of this article were defrayed in part by the payment of page charges. This article must therefore be hereby marked "*advertisement*" in accordance with 18 U.S.C. Section 1734 solely to indicate this fact.

[1] To whom correspondence should be addressed. Tel.: 31-317-482-862; Fax: 31-317-484-801; E-mail: ton.visser@wur.nl.

[2] The abbreviations used are: spFRET, single-pair Förster resonance energy transfer; PHBH, *p*-hydroxybenzoate hydroxylase; POHB, *p*-hydroxybenzoate; FCS, fluorescence correlation spectroscopy; Alexa488, Alexa Fluo 488; Alexa546, Alexa Fluo 546.

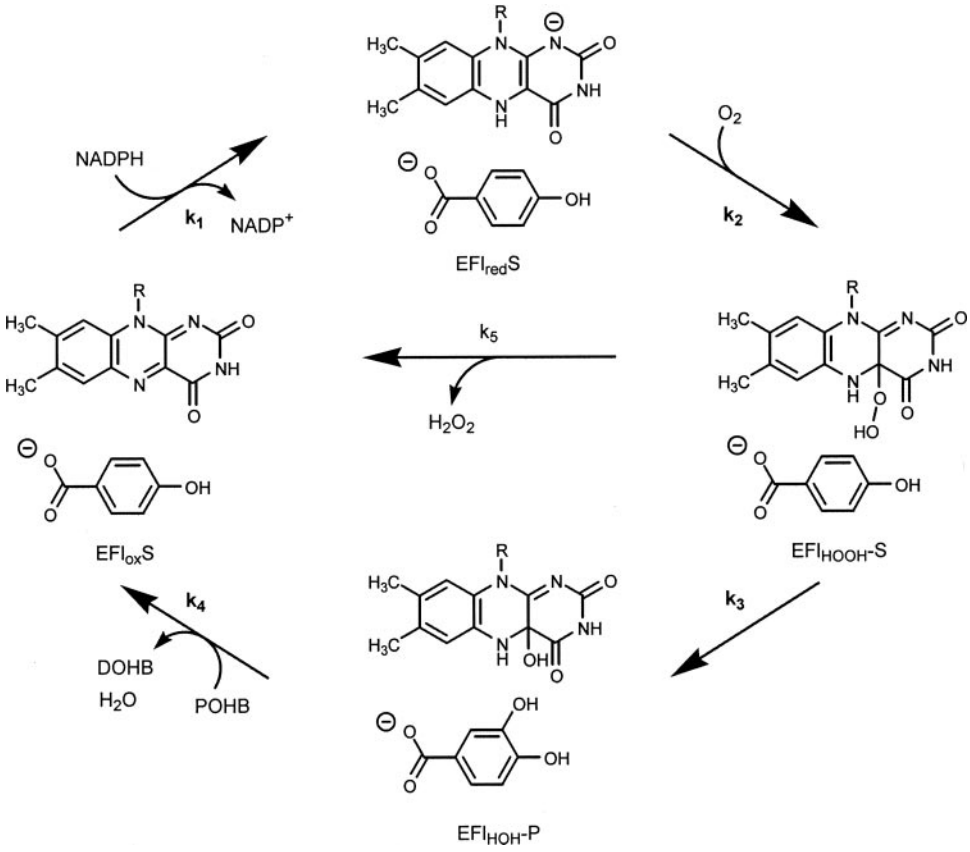

FIGURE 1. **Reaction scheme of PHBH.** $EFl_{ox}S$: oxidized enzyme/substrate complex, EFl_{red}-S: reduced enzyme/substrate complex, EFl_{HOOH}-S: flavin (C4a)-hydroperoxide/substrate complex, EFl_{HOH}-P: flavin (C4a)-hydroxide/product complex, POHB: *p*-hydroxybenzoate, DOHB: 3,4-dihgdroxybenzoate.

oxygen but might transiently be formed for sequestering *p*-hydroxybenzoate to initiate catalysis (26).

PHBH from *Pseudomonas fluorescens* contains five sulfhydryl groups per monomer. However, Cys-116 is the only thiol accessible to labeling with maleimide derivatives (27, 28). Oxidation (28) or mutation (29) of Cys-116 does not influence catalysis but prohibits the reaction with maleimides. We have labeled Cys-116 of PHBH with two different fluorescent maleimides. One fluorescent maleimide used, Alexa Fluo 488 (Alexa488), shows overlap between its fluorescence spectrum and the absorption spectrum of the flavin prosthetic group, whereas the other fluorescent probe used, Alexa Fluo 546 (Alexa546), does not have this spectral overlap and can serve as a control. A three-dimensional representation of dimeric PHBH labeled with the Alexa488 dye is given in Fig. 2. The distance between Alexa488 and the isoalloxazine ring of the FAD within the same subunit amounts to 39 Å.

The experiments conducted with this system are 2-fold: time-resolved fluorescence and fluorescence correlation spectroscopy (FCS) measurements of the labeled enzymes in the absence and presence of enzymatic turnover. The results of these experiments show, for the first time, the suitability of the followed approach. The time-resolved fluorescence measurements on an ensemble of enzyme molecules provided a proof of principle. The single-molecule FCS experiments on PHBH under turnover conditions revealed distinct time-dependent fluorescence intensity fluctuations.

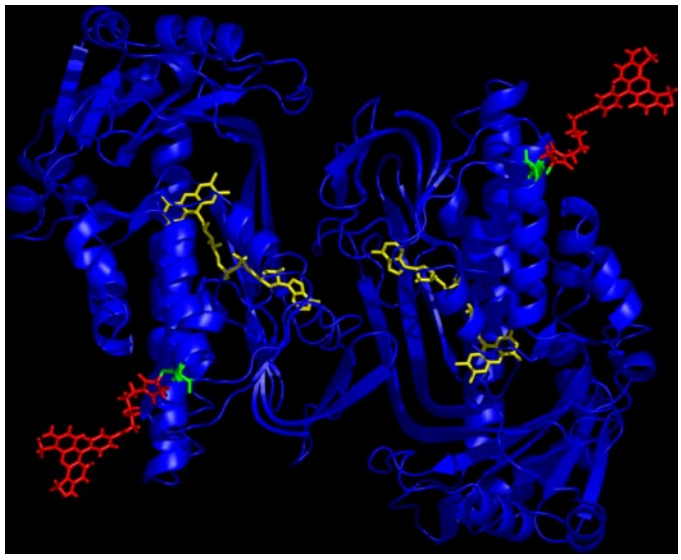

FIGURE 2. **Crystal structure of the enzyme-substrate complex of PHBH (25, 51) showing the FAD in *yellow* and modeled Alexa488 in *red*.**

EXPERIMENTAL PROCEDURES

Materials—Rhodamine 110, tetramethyl-rhodamine, and Alexa488- and Alexa546-maleimides were purchased from Molecular Probes Europe BV (Leiden, The Netherlands). NADPH was obtained from Roche Diagnostics (Mannheim, Germany). All other chemicals used were of the highest purity available. Buffers were made from nanopure-grade water (Millipore, Billerica, MA) and before use were filtered through a 0.22-μm filter (Millipore).

Labeled Protein Preparation—Recombinant PHBH was expressed and purified as described previously (30). The enzyme was pure as judged by SDS-PAGE and stored at −70 °C in 50 mM potassium phosphate buffer, pH 7.0, containing 0.5 mM EDTA and 0.5 mM dithiothreitol. Immediately before labeling, dithiothreitol was removed by gel filtration on a Bio-Gel P-6DG column (Bio-Rad), equilibrated in 50 mM potassium phosphate buffer, pH 7.0, containing 0.5 mM EDTA. Male-

imide labeling of PHBH was carried out using the protocol provided by Molecular Probes. Excess of free label was removed by gel filtration on Superdex 200 HR 10/30 (Amersham Biosciences) in 10 mM potassium phosphate buffer, 0.5 mM EDTA (pH 7.0). The labeled enzyme was directly used in experiments, because it was noticed that prolonged standing resulted in the formation of aggregates and loss of activity. All spectroscopic measurements were carried out in 10 mM potassium phosphate buffer, 0.5 mM EDTA, pH 7.0 at 20 °C.

The degree of labeling was determined by comparison of the absorption spectra of unlabeled PHBH and Alexa488- or Alexa546-labeled PHBH. The concentrations of protein-bound dye were determined by using molar absorption coefficients $\epsilon_{554} = 93\ \mathrm{mM^{-1}\ cm^{-1}}$ and $\epsilon_{493} = 72\ \mathrm{mM^{-1}\ cm^{-1}}$ for Alexa546 and Alexa488, respectively, and a molar absorption coefficient ϵ_{450} of 10.2 $\mathrm{mM^{-1}\ cm^{-1}}$ (30) for the unlabeled protein. For Alexa488-PHBH conjugates, the Bradford protein assay method was used to determine the protein content. Native PHBH served as a reference to obtain a calibration curve. The degree of labeling was also established by mass spectrometry. For this, 2 μM enzyme in 10 mM ammonium acetate, pH 6.8, was introduced in a nanoflow electrospray mass spectrometer coupled to an orthogonal time-of-flight analyzer operating in positive ion mode (Micromass LC-T, Waters). Preparation of nanoflow capillaries and optimization of the electrospray voltages was as described in Ref. 31.

Enzyme Activity—PHBH activity was measured in air-saturated 100 mM Tris/sulfate, pH 8.0, containing 0.5 mM EDTA, 200 μM *p*-hydroxybenzoate (POHB) and 200 μM NADPH (32). The rate of NADPH oxidation was followed by recording the absorption decrease at 340 nm. Enzyme concentrations were determined by using a molar absorption coefficient ϵ_{450} of 10.2 $\mathrm{mM^{-1}\ cm^{-1}}$ (30).

Spectral Measurements—Light absorption measurements were performed on a Hewlett-Packard HP 8453 diode array spectrophotometer. Corrected fluorescence spectra were obtained using a Horiba Jobin Yvon Fluorolog 3.2.2 spectrofluorometer. To compare the fluorescence quantum yields of Alexa488 in water (pH 7.0) with that of fluorescein in 0.1 M sodium hydroxide in water, the absorbance of both solutions was made equal at the excitation wavelength of 480 nm, and the emission spectra were integrated.

Time-resolved Fluorescence—Time-resolved fluorescence experiments were performed using the single-photon timing technique with pulsed laser excitation as recently described (33). The laser repetition frequency amounted to 3.8×10^6 pulses per second, the maximum pulse energy was at the sub-pJ level, the wavelength was 488 nm, and the pulse duration was ~0.5 ps. Quartz cuvettes (1-cm path length in excitation, 1-ml volume) were placed in a thermostatted holder (20 °C). Fluorescence light was detected at an angle of 90° relative to the laser beam and passed through a combination of an OG 530 cut-off filter (Schott, Mainz, Germany) and a 526 nm band-pass filter ($\Delta\lambda$ = 12.6 nm, Schott) or a 570.3 nm band-pass filter ($\Delta\lambda$ = 10.3 nm, Schott) for Alexa488- and Alexa546-PHBH samples, respectively. The concentration of the labeled enzymes amounted to 200 nM. All measurements consisted of a number of sequences of measuring intervals of 10-s parallel ($I_\parallel$) and of 10-s perpendicular ($I_\perp$) polarized emission for a total of ~2 min for each sample. For experimental decay, 4096 channels were used with a time spacing of 8.3 ps per channel. Erythrosine B in nanopure water (with a known single lifetime of 80 ps) served as a reference compound to yield the dynamical instrumental response curve (34).

Fluorescence Intensity Decay Analysis—The total fluorescence intensity decay $I(t)$ is obtained from the measured parallel $I_\parallel(t)$ and perpendicular $I_\perp(t)$ fluorescence intensity components relative to the polarization direction of the exciting beam through the relation,

$$I(t) = I_\parallel(t) + 2I_\perp(t) \qquad \text{(Eq. 1)}$$

The fluorescence lifetime profile consisting of a sum of discrete exponentials with lifetime τ_i and amplitude α_i can be retrieved from the total fluorescence $I(t)$ through the convolution product with the instrumental response function $E(t)$ according to Equation 2.

$$I(t) = E(t) \otimes \sum_{i=1}^{N} \alpha_i e^{-t/\tau_i} \qquad \text{(Eq. 2)}$$

Data analysis with a model of discrete exponential terms was performed using the TRFA Data Processing Package version 1.2 of the Scientific Software Technologies Center (Belarusian State University, Minsk, Belarus, www.sstcenter.com) (details in Refs. 33 and 35).

Fluorescence Anisotropy Decay Analysis—In time-resolved fluorescence anisotropy experiments the angular displacement of fluorophore emission dipoles is measured in real-time. The experimental observable is the fluorescence anisotropy r defined as in Equation 3.

$$r(t) = \frac{I_\parallel(t) - I_\perp(t)}{I_\parallel(t) + 2I_\perp(t)} \qquad \text{(Eq. 3)}$$

The anisotropy decay of proteins is often affected by rapid reorientation of the fluorophore in addition to the much slower overall rotation of the protein. This applies for both internal and external fluorophores attached to the protein. The anisotropy decay of a protein exhibiting rapid internal reorientation and slow overall rotation can be described by Equation 4 (36).

$$r(t) = \{\beta_1 \exp(-t/\phi_{\mathrm{int}}) + \beta_2\}\exp(-t/\phi_{\mathrm{prot}}) \qquad \text{(Eq. 4)}$$

Here the parameter ϕ_{int} is the time constant for rapid internal reorientation, ϕ_{prot} is the rotational correlation time of the protein, and $\beta_1 + \beta_2$ is the fundamental anisotropy. We can define a second-rank order parameter S for a fluorophore reorienting in a protein according to Equation 5.

$$S^2 = \frac{\beta_2}{\beta_1 + \beta_2} = \frac{1}{2}\cos\psi(\cos\psi + 1) \qquad \text{(Eq. 5)}$$

The parameter ψ is the angular displacement of the fluorophore due to internal reorientation. It can be immediately seen that $S = 1$ when there is no flexibility ($\beta_1 = 0$). The rate of reorientation is given by the diffusion coefficient $D_\perp$ of internal motion (Equation 6) (36).

$$D_\perp = \frac{1 - S^2}{6\phi_{\mathrm{int}}} \qquad \text{(Eq. 6)}$$

Data analysis was performed using the TRFA Data Processing Package version 1.2 of the Scientific Software Technologies Center (Belarusian State University) (details in Refs. 33, 35, and 37).

Fluorescence Correlation Spectroscopy—The setup for performing FCS was basically as described in detail elsewhere (38). All measurements were performed with a Zeiss LSM ConfoCor 2 combined microscope system (Carl Zeiss, Jena, Germany). For excitation of the Alexa488-PHBH conjugate, the 488 nm line of an air-cooled argon ion laser was used. For excitation of the Alexa546-PHBH conjugate, the 543

nm laser line of a helium-neon laser was used. The laser power was set at 2.5 microwatts of output for the 488 nm line and at 1.5 microwatts for the 543 nm line, yielding good signal-to-noise autocorrelation traces and low triplet-state contribution (39). A sample of rhodamine 110 (488 nm excitation) or tetramethylrhodamine (543 nm excitation) in nanopure water was used for calibration of the beam profile characterized by the structural parameter *sp* of the three-dimensional Gaussian-shaped observation volume ($sp = \omega_z/\omega_{xy}$; ω_z and ω_{xy} are the axial and equatorial radii, respectively). The beam radius (ω_{xy}) can be determined from the measured diffusion time (τ_D) and the known diffusion coefficients (D) of rhodamine 110 ($D = 280\ \mu m^2/s$) and tetramethylrhodamine ($D = 260\ \mu m^2/s$) applying Equation 7.

$$\tau_D = \omega_{xy}^2/4D \qquad \text{(Eq. 7)}$$

Typical values obtained from calibration with rhodamine 110 are $\tau_D = 16\ \mu s$ and $S = 4.8$ and with tetramethylrhodamine $\tau_D = 50\ \mu s$ and $S = 8.4$. Samples were placed in 8-chambered plates (Nunc, Rochester, NY) with borosilicate bottom. Enzyme concentrations were 10–50 nM, and substrate concentrations were the same as those used for PHBH activity assays. Autocorrelation traces were acquired 10 times with 30-s periods.

FCS Analysis—The autocorrelation curves were globally analyzed to specified models by using the FCS Data Processor version 1.4 of the Scientific Software Technologies Center (Belarusian State University) (40). In global analysis, several correlation curves are combined in one data set and simultaneously fitted with certain parameters linked over the set ensuring more reliable parameter recovery.

Two model functions were used to fit the experimental autocorrelation curves. The first model is that of three-dimensional diffusion and triplet-state relaxation according to,

$$G_{before}(\tau) = 1 + \frac{1}{N}\cdot\frac{1 - A + A\exp(-\tau/\tau_T)}{(1-A)} \cdot 1/((1 + (\tau/\tau_D))\sqrt{1 + (\tau/sp^2\tau_D)}) \qquad \text{(Eq. 8)}$$

where G_{before} is the model function before enzymatic reaction, N is the number of fluorescent molecules in the observation volume, $t\tau_D$ is the diffusion time, τ_T is the triplet-state lifetime, A is the triplet-state fraction, and *sp* is the structural parameter. The second model is that of three-dimensional diffusion model, triplet-state kinetics and an additional exponential relaxation process with relaxation time τ_R and associated amplitude B according to,

$$G_{reaction}(\tau) = 1 + \frac{1}{N}\cdot\frac{1 - A + A\exp(-\tau/\tau_T)}{(1 - A)} \cdot \frac{1 - B + B\exp(-\tau/\tau_R)}{(1 - B)} \cdot 1/((1 + (\tau/\tau_D))\sqrt{1 + (\tau/sp^2\tau_D)}) \qquad \text{(Eq. 9)}$$

where $G_{reaction}$ is the model function applicable during enzymatic reaction.

RESULTS

Properties of Labeled Enzyme—The enzyme labeled with either dye had an activity of 54 ± 2 units per mg of protein, which is comparable to that of the wild-type enzyme (28). Comparison of absorption spectra of unlabeled enzyme and labeled enzyme indicated an almost 100% labeling efficiency (results not shown). Nanoflow electrospray ionization mass spectroscopy revealed that Alexa488-PHBH contained ~0.95 mol of dye per subunit. Moreover, under optimal spray conditions (31), Alexa488-PHBH was almost completely in the dimeric holo- form with a mass of 91,633 ± 30 Da. The minor monomeric fraction of Alexa488-PHBH gave a mass of 45,810 ± 10 Da. These values are in good agreement with the reported masses of C116S-PHBH (dimer mass = 90,233 ± 30 Da; monomer mass = 45,096 ± 6 Da; sequential mass = 45,090.7 with FAD) (29) and taking the mass of the free Alexa488 dye (mass = 721) into account.

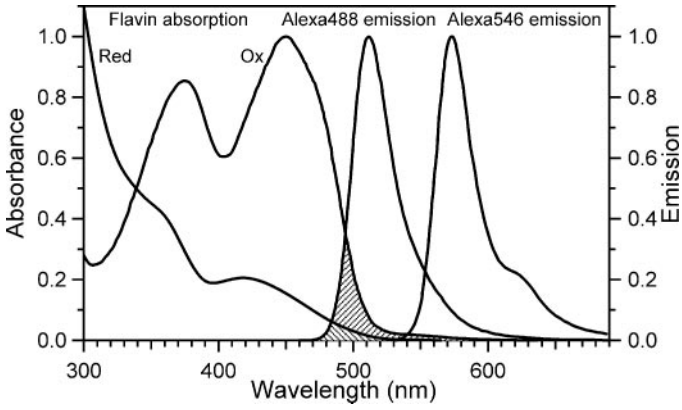

FIGURE 3. **Absorption spectra of oxidized and reduced FAD in PHBH and fluorescence emission spectra of Alexa488 and Alexa546 covalently attached to PHBH.** The spectra are normalized. The *dashed areas* show the overlap between FAD absorption spectra (oxidized/reduced) and the Alexa488 fluorescence emission spectrum.

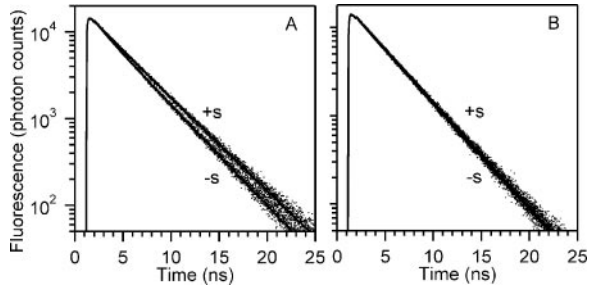

FIGURE 4. **Experimental (*dots*) and fitted (*solid line*) fluorescence decays obtained from single-photon timing of Alexa488 covalently coupled to PHBH (*A*) and of Alexa546 covalently coupled to PHBH (*B*).** Two sets of normalized curves are shown: before reaction (−*s*) and during reaction (+*s*). The obtained parameters are collected in Table 1. All reduced χ^2 values are between 1.1 and 1.2 indicating excellent fits.

Fig. 3 shows the absorption spectrum of oxidized and reduced FAD in PHBH and the fluorescence emission spectra of Alexa488 and Alexa546. There is a clear spectral overlap between the FAD absorption spectrum and the Alexa488 fluorescence emission spectrum, whereas this overlap does not exist in case of Alexa546 as donor. The absorption spectra of the reduced and oxygenated FAD species formed during PHBH catalysis show reduced absorption peaks and are more UV-shifted than the absorption spectrum of oxidized FAD (41); they have strongly reduced overlap with the fluorescence spectrum of Alexa488. The critical transfer distance (42) is obtained from,

$$R_0 = 0.211[\kappa^2 n^{-4} Q_D J(\lambda)]^{(1/6)} \qquad \text{(Eq. 10)}$$

where κ^2 is the dipole orientation factor taken as 2/3 (dynamical average limit), n is the refractive index ($n = 1.33$), Q_D is the quantum yield of donor fluorescence ($Q_D = 0.85$ for Alexa488; by comparison to $Q_D = 0.92$ of fluorescein in 0.1 M sodium hydroxide in water), and $J(\lambda)$ is the spectral overlap integral ($6.68 \times 10^{13}\ M^{-1}\ cm^{-1} nm^4$). R_0 is calculated to be 32 Å.

The efficiency of resonance energy transfer E as function of the

TABLE 1
Fluorescence decay parameters of Alexa488 and Alexa546 dyes covalently attached to PHBH

Enzyme	α_1[a]	τ_1[a]	α_2[a]	τ_2[a]	$\langle\tau\rangle$[b]
		ns		*ns*	*ns*
Alexa488-PHBH+POHB	0.18 (0.17–0.20)[c]	0.92 (0.74–1.07)	0.82 (0.81–0.83)	3.70 (3.69–3.73)	3.20 (3.16–3.25)
Alexa488-PHBH+POHB+NADPH	0.15 (0.14–0.17)	0.82 (0.65–1.00)	0.85 (0.83–0.86)	4.00 (3.99–4.02)	3.52 (3.49–3.57)
Alexa546-PHBH+POHB	0.13 (0.10–0.18)	0.27 (0.15–0.44)	0.87 (0.87–0.88)	3.59 (3.56–3.62)	3.16 (3.12–3.21)
Alexa546-PHBH+POHB+NADPH	0.15 (0.14–0.18)	0.50 (0.36–0.66)	0.85 (0.83–0.86)	3.57 (3.56–3.60)	3.11 (3.08–3.16)

[a] α_1, τ_1, α_2, and τ_2 are defined in Equation 2.
[b] The average lifetime is defined as $\langle\tau\rangle = \alpha_1\tau_1 + \alpha_2\tau_2$, with $\alpha_1 + \alpha_2 = 1$.
[c] Values in parentheses were obtained after a rigorous error analysis at the 0.67 confidence level.

relative distance R/R_0 (R is the actual distance, 39 Å) is obtained from Equation 11.

$$E = \frac{1}{1 + (R/R_0)^6} \qquad \text{(Eq. 11)}$$

Having established both actual and Förster distances, the efficiency of transfer from Alexa488 to FAD is calculated to be 23%. For the reduced and oxygenated FAD species the spectral overlap integral is much less (0.99×10^{13} M^{-1} cm^{-1} nm^4, R_0 = 23 Å) leading to a transfer efficiency of only 3%. The distance of the FAD cofactor of one protein subunit to the Alexa488 molecule in the other protein subunit (57 Å) is much larger than the one in its own subunit (39 Å), yielding an efficiency of transfer of 3% from Alexa488 to the oxidized FAD in the other subunit.

Fluorescence Intensity Decay—We have carried out time-resolved fluorescence experiments on Alexa488-PHBH and Alexa546-PHBH under conditions where either one of the substrates (NADPH or POHB) is present or during catalysis when both substrates are present. Fig. 4*A* shows the fluorescence decay results of Alexa488 labeled PHBH (200 nM) before and during reaction.

The best fit to the experimental data were a bi-exponential function with a dominant longer lifetime component (Table 1). The most striking result is that the fluorescence decay becomes longer during the reaction. This observation is in line with the fact that resonance energy transfer is diminished during the reaction, because the FAD is reduced or oxygenated; the absorption spectra exhibit much less overlap with the donor emission spectrum. During the fluorescence decay experiments taken under enzymatic turnover conditions the flavin in PHBH is alternating between different redox or FRET states. The control experiment with 200 nM Alexa546-PHBH (Fig. 4*B* and Table 1) shows fluorescence decays that are unaffected during the reaction (average lifetimes, $\langle\tau\rangle$, are 3.16 and 3.11 ns). The order of substrate addition does not influence the decay patterns (results not shown). From the average lifetimes obtained before ($\langle\tau\rangle_{\text{before}}$ = 3.20 ns) and during ($\langle\tau\rangle_{\text{reaction}}$ = 3.52 ns) reaction with Alexa488-PHBH, the relative transfer efficiency E can be determined from Equation 12.

$$E = 1 - \langle\tau\rangle_{\text{before}}/\langle\tau\rangle_{\text{reaction}} \qquad \text{(Eq. 12)}$$

E calculated from Equation 12 amounted to 10%. The apparent discrepancy with the calculated, distance-based transfer efficiency (23%) can be explained by switching of the Alexa488 donor probe between longer (no FRET) and shorter (FRET) lifetimes leading to an average lifetime that is shorter than expected. In addition, during the measuring time the substrates are depleted leading to an average fluorescence lifetime that is more weighted to the shorter lifetime.

Fluorescence Anisotropy Decay—In Fig. 5 an example of the experimental and fitted fluorescence anisotropy decays of Alexa488-PHBH

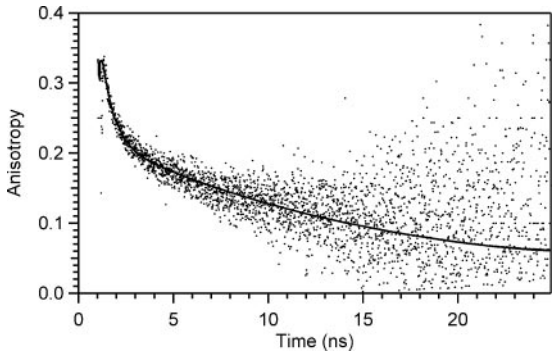

FIGURE 5. **Example of experimental (*dots*) and fitted (*solid line*) fluorescence anisotropy decay of Alexa488 covalently coupled to PHBH in the presence of NADPH and POHB.** The obtained decay parameters of all anisotropy experiments are collected in Table 2.

(200 nM) is shown. It can be clearly observed that the anisotropy decay is composed of a rapid component and a slow component. The rapid process arises from fast internal motion of the Alexa488 label superimposed on the slower overall protein rotation. The results of analysis of all protein experiments are collected in Table 2.

Fluorescence Correlation Spectroscopy—FCS is an established technique for measuring fluorescence intensity fluctuations arising from changes in the number of fluorophores due to diffusion or chemical reaction in a tiny open observation volume (<1 fl) under equilibrium conditions (43). Typical autocorrelation traces of Alexa488-PHBH (23 nM) in the absence and presence of substrates are shown in Fig. 6. Adding first POHB to the enzyme followed by NADPH gave identical results as adding the substrates in reversed order. NADPH or POHB or the combination of both did not give any background fluorescence signal when measured separately. The experimental curves before reaction were globally analyzed by using a model of three-dimensional diffusion and triplet-state kinetics (Equation 8). When the FCS measurements were done during enzymatic turnover conditions, the experimental autocorrelation curves could only be properly fitted to a three-dimensional diffusion model with triplet-state kinetics and an additional exponential relaxation process (Equation 9). The difference in fit quality with and without the extra relaxation component is clearly visible in Fig. 6, showing experimental, fitted, and residuals traces obtained before and just after start of catalysis. Global analysis linking the diffusion times and triplet parameters over the complete data set and the relaxation times only in the subset of measurements obtained during turnover conditions yielded parameters that are collected in Table 3. In Table 3 diffusion coefficients D are listed that are calculated by using Equation 7.

During reaction, the number of enzyme molecules appears to change, as is visible in the traces shown in Fig. 6. The amplitude of the autocor-

TABLE 2
Fluorescence anisotropy decay analysis of Alexa488 and Alexa546 dyes covalently attached to PHBH

Enzyme	β_1[a]	ϕ_{int}[a]	β_2[a]	ϕ_{prot}[a]	ψ[a]	$D_\perp$[a]
		ns		*ns*	*degrees*	ns^{-1}
Alexa488-PHBH+POHB	0.112 (0.108–0.116)[b]	0.63 (0.56–0.69)	0.198 (0.195–0.203)	15.4 (14.5–16.1)	42.6 (42.3–42.8)	0.096 (0.088–0.106)
Alexa488-PHBH+POHB+NADPH	0.115 (0.111–0.119)	0.60 (0.54–0.66)	0.201 (0.197–0.203)	17.5 (16.6–18.3)	42.9 (42.6–43.2)	0.101 (0.093–0.111)
Alexa546-PHBH+POHB	0.074 (0.068–0.081)	1.33 (1.09–1.63)	0.262 (0.258–0.275)	22.4 (20.9–24.5)	32.3 (31.4–32.9)	0.028 (0.023–0.032)
Alexa546-PHBH+POHB+NADPH	0.078 (0.072–0.085)	1.32 (1.10–1.55)	0.262 (0.254–0.269)	22.0 (20.5–23.7)	33.0 (32.4–33.9)	0.029 (0.026–0.033)

[a] β_1, ϕ_{int}, β_2, ϕ_{prot}, ψ and $D_\perp$ are defined in Equations 4–6.
[b] Values in parentheses were obtained after a rigorous error analysis at the 0.67 confidence level.

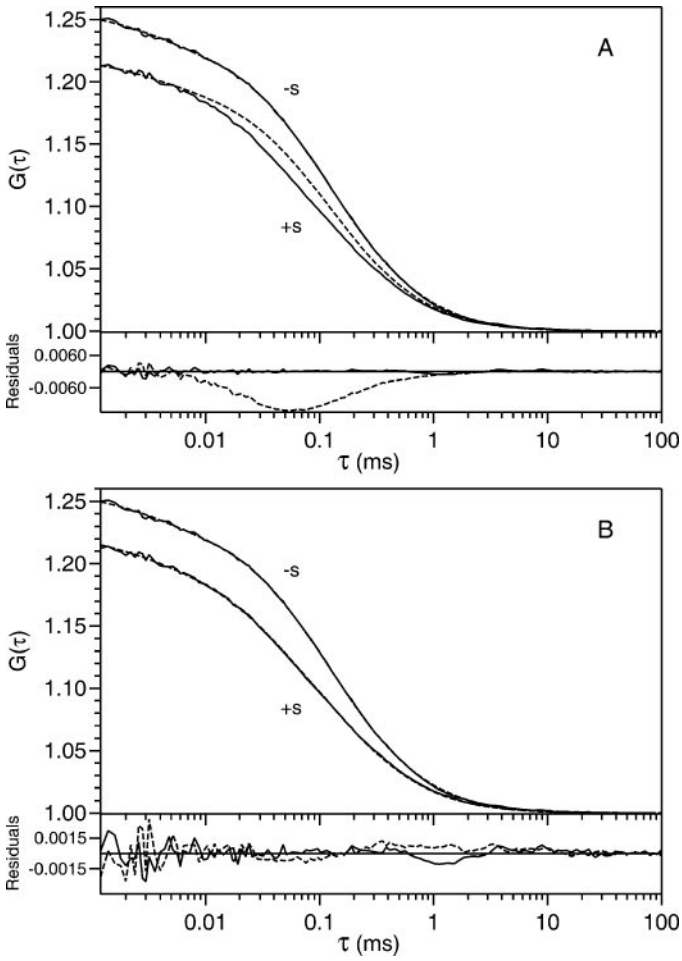

FIGURE 6. **Representative experimental (*dashed line*) and fitted (*solid line*) autocorrelation traces obtained from FCS experiments with Alexa488-PHBH (22. 8 nM) in the presence of NADPH before reaction (−*s*) and during reaction upon addition of POHB (+*s*).** *A*, the experimental data points before reaction (−*s*) and during reaction (+*s*) were globally analyzed according to a one-component three-dimensional diffusion model with triplet kinetics (Equation 8). *B*, the experimental data points during reaction (+*s*) were also globally analyzed to the same model extended with a relaxation part (Equation 9). The triplet lifetimes and fractions were linked over the appropriate data sets. The quality of the fit is indicated in plots of the residuals. Note the bad fit of the experimental data during reaction (+*s*) in *panel A* (*dashed line*). The obtained parameters of all FCS experiments are collected in Table 3.

relation function $G(0)$ is proportional to $1 + 1/N$. The lower values for $G(0)$ during reaction indicate an increase in the number of molecules observed. When the enzyme concentration was varied from 10 to 50 nM in similar separate FCS experiments, the relative increase in number of molecules ($\Delta N/N$) became less (50% to 10% increase, respectively) (Fig. 7). Similar results on the relative change in number of molecules were obtained for FCS experiments on Alexa546-PHBH at different concentrations (results not shown). These observations are indicative for a dimer-monomer equilibrium that is affected during catalysis.

When autocorrelation traces were recorded in time during the reaction, the extra relaxation component disappeared again when the substrates were depleted. The time for the disappearance (4–5 min) was in good agreement with the duration of the reaction for the amounts of enzyme and substrates used. The number of molecules also decreased again but did not come completely back to the level before the start of the reaction.

The measured diffusion time of the Alexa488-labeled enzyme during turnover is a little shorter, 115 μs compared with 126 μs without substrates. The theoretical diffusion time for a monomer is 1.26 times shorter than that of a dimeric, spherical particle. We find approximately a 1.15 times shorter diffusion time during turnover conditions for both labeled enzymes. It should be realized, however, that these differences fall within the confidence limits of the recovered parameters (Table 3). This is in agreement with the limited mass resolution of fluorescence correlation measurements (44).

DISCUSSION

We studied the ensemble-averaged fluorescence lifetimes of Alexa-labeled PHBH (200 nM) in the resting state and under catalytic turnover conditions (see Table 1 and Fig. 4). A proof of principle was obtained for observing catalytic events, because the average lifetime of Alexa488-PHBH becomes longer under turnover conditions (Fig. 4*A*). The average lifetime of Alexa546-PHBH does not change during catalysis (Fig. 4*B*). This lengthening of the fluorescence lifetime is due to the fact that catalysis is accompanied by modulation of resonance energy transfer from Alexa488 to FAD. The longest fluorescence lifetime without resonance energy transfer would be expected in the range of 4.5 ns. An average lifetime of 3.5 ns is found because the enzyme predominantly exists in the oxidized, resting state ($\langle\tau\rangle = 3.2$ ns) and, after a few minutes of reaction, substrates are depleted and the reaction is terminated.

The choice for a random orientation factor ($\kappa^2 = 2/3$) in the calculation of the critical transfer distance (R_0) can be validated. From time-resolved fluorescence anisotropy of Alexa488-PHBH, we found that the Alexa dye (donor) is very flexibly attached to the protein showing a wobbling frequency of 100 MHz and angular displacement of ~43° (see Table 2 and Fig. 5). This result is in agreement with electron spin resonance studies of PHBH equipped with maleimide spin-label derivatives (28) indicating flexibly bound spin labels on the protein surface. In addition, during catalysis the isoalloxazine ring of the FAD cofactor (acceptor) is moving in and out of the active site (20, 21). Both types of movement contribute to randomization of the transition dipoles of donor and acceptor. Both labels have slightly different rotational dynamic properties (Table 2). Alexa546 is more rigidly bound to the enzyme than Alexa488. This difference is probably due to the different molecular structures of both labels. Alexa546 possesses a larger chromophoric

TABLE 3
FCS parameters of Alexa488 and Alexa546 dyes covalently attached to PHBH

Enzyme	Model[a]	A[a]	τ_T[a]	B[a]	τ_R[a]	τ_D[a]	D[b]
		%	μs	%	μs		$\mu m^2/s$
Alexa488-PHBH+NADPH	Diffusion	8.0 (6.8–9.6)[d]	2.4 (1.7–3.3)	NA[c]	NA	126 (112–138)	35.8 (32.7–40.3)
Alexa488-PHBH+NADPH+POHB	Diffusion + relaxation	8.0 (6.4–10.1)	2.8 (2.1–3.6)	15.8 (14.1–17.3)	22.8 (19.8–26.0)	115 (101–127)	39.2 (36.1–43.3)
Alexa546-PHBH+NADPH	Diffusion	4.9 (3.6–7.0)	5.8 (2.6–9.0)	NA	NA	377 (369–381)	34.7 (34.3–35.5)
Alexa546-PHBH+NADPH+POHB	Diffusion	5.8 (5.2–6.5)	7.0 (5.4–9.3)	NA	NA	368 (358–379)	35.5 (34.5–36.5)

[a] Model used for fitting the data: diffusion plus triplet (Equation 8); diffusion plus triplet plus relaxation (Equation 9); A, B, τ_T, τ_R, and τ_D are defined in Equations 8 and 9.
[b] D is the diffusion coefficient obtained from Equation 7.
[c] NA, not applicable.
[d] Values in parentheses are obtained after a rigorous error analysis at the 0.67 confidence level.

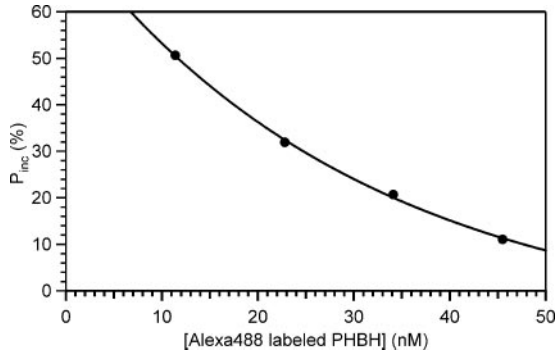

FIGURE 7. **Alexa488-PHBH concentration-dependent change in number of molecules calculated from autocorrelation traces obtained in FCS experiments.** Percentage increase is calculated using $P_{inc} = (N_{+S} - N_{-S})/N_{-S}) \times 100$; N_{+S} = number of molecules during reaction, and N_{-S} = number of molecules before starting the reaction.

group, has a longer side chain, and might fold back on the protein surface.

FCS experiments focus on the properties of single enzyme molecules. The autocorrelation curves of Alexa488-PHBH under turnover conditions could be well described using the diffusion-relaxation model of Equation 9 assuming a chemical relaxation process with relaxation time τ_R (see Table 3 and Fig. 6). The relaxation process must originate from one that causes fluorescence intensity fluctuations. During enzymatic turnover the flavin shuttles between two redox states that is sensed by the Alexa488 fluorescence emitting 77% of its maximum because of resonance energy transfer to flavin in the oxidized state and 97% when the flavin is reduced. The effect is small, as illustrated by values of the amplitude B (16%), but significant. As expected, control FCS measurements with Alexa546-PHBH yielded experimental autocorrelation curves that could be perfectly fitted by using Equation 8, irrespective of enzymatic turnover. Because this effect is not observed with Alexa546-PHBH, it should originate from limited blinking of Alexa488 fluorescence due to modulation of resonance energy transfer during catalysis. Therefore, the relaxation time $\tau_R \approx 23$ μs is connected to the equilibrium of PHBH in oxidized and reduced forms and the rate constant is equal to,

$$1/\tau_R = k_R = k_{ox} + k_{red} \qquad \text{(Eq. 13)}$$

where k_{ox} and k_{red} are the rate constants for the oxidative and reductive half reactions. The relaxation rate constant $k_R = 4.4 \times 10^4\ s^{-1}$. This rate is a thousand times larger than the turnover rate of the enzyme, which is $\sim 37\ s^{-1}$ under the conditions applied (45).

During PHBH catalysis, the isoalloxazine ring of the FAD alternates between the two active sites (26). In the oxidized state, the flavin swings *out* for the reaction with NADPH, whereas in the reduced form, the flavin occupies the *in* position, which is protected from bulk solvent. The oxygenated flavin intermediates formed during the PHBH reaction cycle (Fig. 1) are not good acceptors for resonance energy transfer from Alexa488 because of diminished spectral overlap (41). Therefore, it is tempting to associate the observed relaxation rate to a conformational event related to the *in* and *out* transition of the isoalloxazine ring of the FAD. Alternatively, it might reflect the transient formation of the *open* conformation, which seems required for substrate binding and product release (24, 26).

Very recently, single-molecule fluorescence studies monitoring isoalloxazine fluorescence of agarose-immobilized PHBH in the absence of substrates were reported (46). From the single-molecule trajectories, evidence was obtained for dynamic motions of the flavin between "in" and "out" conformations of the enzyme on the time scale of tens of milliseconds. Other examples of the intimate linkage between enzyme conformational dynamics and catalysis have been recently found using both single-molecule kinetic investigations of dihydrofolate reductase (14) and nuclear magnetic resonance relaxation methods on cyclophilin A ensembles (47, 48).

A comparable microsecond-relaxation dynamics study using FCS was reported for the intestinal fatty acid binding protein (15 kDa) by using fluorescence self-quenching as source of fluorescence intensity fluctuations (49, 50). The fluctuations of the fluorescence have been used as a reporter of the fluctuations in the structure, and conformational events with characteristic relaxation times of 1–40 μs were measured depending on the folding state of the protein.

The FCS experiments show that during reaction the number of enzyme molecules initially increases. PHBH is a dimeric protein. Therefore, the increase can be explained by a dimer-monomer equilibrium, which is shifted more to the monomer side during reaction thereby yielding more molecules. The involvement of such equilibrium is in agreement with the observation that at higher enzyme concentrations the difference between the number of enzyme molecules before and during the reaction becomes smaller (Fig. 7). The measured diffusion time of the enzyme during turnover is also a little shorter, as would be expected for monomer containing samples. The FCS method is actually not very sensitive to 2-fold changes in mass (44). The theoretical diffusion time of a monomer is 1.24 times shorter than that of a dimer. We found a diffusion time that was ~1.15 times shorter during turnover conditions, in agreement with the fact that the enzyme sample consists of a mixture of monomers and dimers.

From the data presented in Fig. 7 a dissociation constant K_d of ~5 nM can be estimated for the dimer-monomer equilibrium. This remarkable observation of dissociation during catalysis has until now not been reported for PHBH, as conventional kinetic and spectroscopic methods cannot be used at these low concentrations. The enzyme is known to dissociate into active monomers by adding Me_2SO (21, 28, 45). The

exact mechanism for this dissociation during catalysis is not clear yet and requires further investigation. Structural changes might reduce the binding interactions in the dimeric interface resulting in a raised dissociation constant, just in the range of our FCS measurements. In the time-resolved fluorescence experiments 200 nM of labeled protein was used, keeping all the PHBH molecules in the dimeric form.

CONCLUDING REMARKS

We have equipped PHBH with a fluorescent Alexa488 dye that can act as sensor for the flavin redox state. The sensing is based on modulation of resonance energy transfer from the Alexa488 dye by the two redox states of the flavin. The Alexa dyes are attached on a site of PHBH that exhibits minimal interference with the active site. The proof of principle was given in ensemble measurements of fluorescence lifetimes showing a small but significant increase when PHBH performs catalysis. In the single photon timing experiments millions of events of many enzyme molecules are monitored during 50-ns periods, much shorter than the real catalytic events. Information is obtained on "pseudo" stationary states of the enzyme. By using fluorescence correlation spectroscopy only a few enzyme molecules transiting during a fraction of a second through a tiny volume are observed, and many are briefly watched. Diffusion is one source of fluctuations, whereas the other one consists of the shuttling of enzyme between oxidized and reduced forms. FCS experiments indicate the presence of a relaxation process of PHBH under turnover conditions with a typical time constant of ~23 μs. Furthermore, an until now unobserved catalysis-induced dissociation of the dimeric PHBH into monomers with a K_d of ~5 nM is suggested by the FCS data.

An interesting development for *in vivo* measurements of flavoenzyme activity would be the genetically encoded expression of an adduct of a flavoenzyme fused with one of the variants of the green fluorescent protein (for instance, blue fluorescent protein or cyan fluorescent protein). Similarly as described for Alexa488-PHBH, the fluorescence emission of the visible fluorescent protein can be used as a sensitive antenna for the redox state and thus enzymatic activity of such flavoenzyme in a living cell.

Acknowledgments—We thank Arie van Hoek, Nina Visser, Ruchira Engel, and Nora Tahallah (Utrecht University) for assistance with time-resolved fluorescence, data analysis, and mass spectrometry analysis.

REFERENCES

1. Weiss, S. (1999) *Science* **283,** 1676–1683
2. Weiss, S. (2000) *Nat. Struct. Biol.* **7,** 724–729
3. Lu, H. P., Xun, L., and Xie, X. S. (1998) *Science* **282,** 1877–1882
4. Xie, X. S., and Lu, H. P. (1999) *J. Biol. Chem.* **274,** 15967–15970
5. Michalet, X., Kapanidis, A. N., Laurence, T., Pinaud, F., Doose, S., Pflughoefft, M., and Weiss, S. (2003) *Annu. Rev. Biophys. Biomol. Struct.* **32,** 161–182
6. Deniz, A., Laurence, T. A., Dahan, M., Chemla, D. S., Schultz, P. G., and Weiss, S. (2001) *Ann. Rev. Phys. Chem.* **52,** 233–253
7. Talaga, D. S., Lau, W. L., Roder, H., Tang, J., Jia, Y., DeGrado, W. F., and Hochstrasser, R. M. (2000) *Proc. Natl. Acad. Sci. U. S. A.* **97,** 13021–13026
8. Ha, T. (2001) *Methods* **25,** 78–86
9. Ha, T., Ting, A. Y., Liang, J., Caldwell, W. B., Deniz, A. A., Chemla, D. S., Schultz, P. G., and Weiss, S. (1999) *Proc. Natl. Acad. Sci. U. S. A.* **96,** 893–898
10. Edman, L., Földes-Papp, Z., Wennmalm, S., and Rigler, R. (1999) *Chem. Phys.* **247,** 11–22
11. Zhuang, X., Bartley, L. E., Babcock, H. P., Russell, R., Ha, T., Herschlag, D., and Chu, S. (2000) *Science* **288,** 2048–2051
12. van Oijen, A. M., Blainey, P. C., Crampton, D. J., Richardson, C. C., Ellenberger, T., and Xie, X. S. (2003) *Science* **301,** 1235–1238
13. Diez, M., Zimmermann, B., Börsch, M., König, M., Schweinberger, E., Steigmiller, S., Reuter, R., Felekyan, S., Kudryavtsev, V., Seidel, C. A. M., and Gräber, P. (2004) *Nature Struct. Biol.* **11,** 135–141
14. Antikainen, N. M., Smiley, R. D., Benkovic, S. J., and Hammes, G. G. (2005) *Biochemistry* **44,** 16835–16843
15. Shi, J., Palfey, B. A., Dertouzos, J., Jensen, K. F., Gafni, A., and Steel, D. (2004) *J. Amer. Chem. Soc.* **126,** 6914–6922
16. van den Berg, P. A. W., Widengren, J., Hink, M. A., Rigler, R., and Visser, A. J. W. G. (2001) *Spectrochim. Acta A* **57,** 2135–2144
17. van den Berg, P. A. W., and Visser, A. J. W. G. (2001) in *New Trends in Fluorescence Spectroscopy: Applications to Chemical and Life Sciences* (Valeur, B., and Brochon, J.-C., eds) pp. 457–485, Springer, Heidelberg, Germany
18. Visser, A. J. W. G., van den Berg, P. A. W., Hink, M. A., and Petushkov, V. N. (2001) in *Fluorescence Correlation Spectroscopy. Theory and Applications* (Rigler, R., and Elson, E. S., eds) pp. 9–24, Springer, Berlin
19. Entsch, B., and van Berkel, W. J. H. (1995) *FASEB J.* **9,** 476–483
20. Schreuder, H. A., Mattevi, A., Obmolova, G., Kalk, K. H., Hol, W. G. J., van der Bolt, F. J. T., and van Berkel, W. J. H. (1994) *Biochemistry* **33,** 10161–10170
21. Gatti, D. L., Palfey, B. A., Lah, M. S., Entsch, B., Massey, V., Ballou, D. P., and Ludwig, M. L. (1994) *Science* **266,** 110–114
22. van Berkel, W. J. H., Eppink, M. H. M., and Schreuder, H. A. (1994) *Protein Sci.* **3,** 2245–2253
23. Eppink, M. H. M., Schreuder, H. A., and van Berkel, W. J. H. (1998) *J. Biol. Chem.* **273,** 21031–21039
24. Wang, J., Ortiz-Maldonado, M., Entsch, B., Massey, V., Ballou, D., and Gatti, D. L. (2002) *Proc. Natl. Acad. Sci. U. S. A.* **99,** 608–613
25. Schreuder, H. A., van der Laan, J. M., Swarte, M. B. A., Kalk, K. H., Hol, W. G. J., and Drenth, J. (1992) *Proteins* **14,** 178–190
26. Entsch, B., Cole, L. J., and Ballou, D. P. (2005) *Arch. Biochem. Biophys.* **433,** 297–311
27. van Berkel, W. J. H., Weijer, W. J., Müller, F., Jekel, P. A., and Beintema, J. J. (1984) *Eur. J. Biochem.* **145,** 245–256
28. van Berkel, W. J. H., and Müller, F. (1987) *Eur. J. Biochem.* **167,** 35–46
29. Eschrich, K., van Berkel, W. J. H., Westphal, A. H., de Kok, A., Mattevi, A., Obmolova, G., Kalk, K. H., and Hol, W. G. J. (1990) *FEBS Lett.* **277,** 197–199
30. van Berkel, W. J. H., Westphal, A. H., Eschrich, K., Eppink, M. H. M., and de Kok, A. (1992) *Eur. J. Biochem.* **210,** 411–419
31. Tahallah, N., Pinkse, M., Maier, C. S., and Heck, A. J. (2001) *Rapid Commun. Mass Spectrom.* **15,** 596–601
32. Müller, F., and van Berkel, W. J. H. (1982) *Eur. J. Biochem.* **128,** 21–27
33. Borst, J. W., Hink, M. A., van Hoek, A., and Visser, A. J. W. G. (2005) *J. Fluoresc.* **15,** 153–160
34. Bastiaens, P. I. H., van Hoek, A., Benen, J. A. E., Brochon, J.-C., and Visser, A. J. W. G. (1992) *Biophys. J.* **63,** 839–853
35. Digris, A. V., Skakun, V. V., Novikov, E. G., van Hoek, A., Claiborne, A., and Visser, A. J. W. G. (1999) *Eur. Biophys. J.* **28,** 526–531
36. Szabo, A. (1984) *J. Chem. Phys.* **81,** 150–167
37. van den Berg, P. A. W., van Hoek, A., and Visser, A. J. W. G. (2004) *Biophys. J.* **87,** 2577–2586
38. Hink, M. A., Borst, J. W., and Visser, A. J. W. G. (2003) *Methods Enzymol.* **361,** 93–112
39. Widengren, J., Mets, Ü., Rigler, R. (1995) *J. Phys. Chem.* **99,** 13368–13379
40. Skakun, V. V., Hink, M. A., Digris, A. V., Engel, R., Novikov, E. G., Apanasovich, V. V., and Visser, A. J. W. G. (2005) *Eur. Biophys. J.* **34,** 323–334
41. Entsch, B., and Ballou, D. P. (1989) *Biochim. Biophys. Acta* **999,** 313–322
42. Lakowicz, J. R. (1999) *Principles of Fluorescence Spectroscopy*, 2nd Ed., Kluwer Academic/Plenum Publishers, New York, p. 369
43. Hess, S. T., Huang, S., Heikal, A. A., and Webb, W. W. (2002) *Biochemistry* **41,** 697–705
44. Meseth, U., Wohland, T., Rigler R., and Vogel, H. (1999) *Biophys. J.* **76,** 1619–1631
45. van Berkel, W. J. H., and Müller, F. (1989) *Eur. J. Biochem.* **179,** 307–314
46. Brender, J. R., Dertouzos, J., Ballou, D. P., Massey, V., Palfey B. A., Entsch, B., Steel, D. G., and Gafni, A. (2005) *J. Am. Chem. Soc.* **127,** 18171–18178
47. Eisenmesser, E. Z., Millet, O., Labeikovsky, W., Korzhnev, D. M., Wolf-Watz, M., Bosco, D. A., Skalicky, J. J., Kay, L. E., and Kern, D. (2005) *Nature* **438,** 117–121
48. Eisenmesser, E. Z., Bosco, D. A., Akke, M., and Kern, D. (2002) *Science* **295,** 1520–1523
49. Chattopadhyay, K., Saffarian, S., Elson, E. L., and Frieden, C. (2002) *Proc. Natl. Acad. Sci. U. S. A.* **99,** 14171–14176
50. Chattopadhyay, K., Elson, E. L., and Frieden, C. (2005) *Proc. Natl. Acad. Sci. U. S. A.* **102,** 2385–2389
51. Schreuder, H. A., Prick, P. A. J., Wierenga, R. K., Vriend, G., Wilson, K. S., Hol, W. G. J., and Drenth, J. (1989) *J. Mol. Biol.* **208,** 679–696